

Doc-Start

Structural bioinformatics

An efficient dual sampling algorithm with Hamming distance filtration

Fenix W. Huang¹, Qijun He¹, Christopher Barrett^{1,4} and Christian M. Reidys^{1,2,3*}

¹ Biocomplexity Institute of Virginia Tech, Blacksburg, VA, USA. ² Department of Mathematics, Virginia Tech, Blacksburg, VA, USA. ³ Thermo Fisher Scientific Fellow in Advanced Systems for Information Biology. ⁴ Department of Computer Science, Virginia Tech, Blacksburg, VA, USA.

*To whom correspondence should be addressed.

Associate Editor: XXXXXXXX

Received on XXXXX; revised on XXXXX; accepted on XXXXX

Abstract

Motivation: Recently, a framework considering RNA sequences and their RNA secondary structures as pairs, led to some information-theoretic perspectives on how the semantics encoded in RNA sequences can be inferred. In this context the pairing arises naturally from the energy model of RNA secondary structures. Fixing the sequence in the pairing produces the RNA energy landscape, whose partition function was discovered by McCaskill. Dually, fixing the structure induces the energy landscape of sequences. The latter has been considered for designing more efficient inverse folding algorithms.

Results: We present here the Hamming distance filtered, dual partition function, together with a Boltzmann sampler using novel dynamic programming routines for the loop-based energy model. The time complexity of the algorithm is $O(h^2n)$, where h, n are Hamming distance and sequence length, respectively, reducing the time complexity of samplers, reported in the literature by $O(n^2)$. We then present two applications, the first being in the context of the evolution of natural sequence-structure pairs of microRNAs and the second constructing neutral paths. The former studies the inverse fold rate (IFR) of sequence-structure pairs, filtered by Hamming distance, observing that such pairs evolve towards higher levels of robustness, i.e., increasing IFR. The latter is an algorithm that construct neutral paths: given two sequences in a neutral network, we employ the sampler in order to construct short paths connecting them, consisting of sequences all contained in the neutral network.

Availability: The source code is freely available at <http://staff.vbi.vt.edu/fenixh/HamSampler.zip>

Contact: duckcr@bi.vt.edu

Supplementary information: Supplementary material containing additional data tables are available at *Bioinformatics* online.

1 Introduction

Ribonucleic acid (RNA) is a polymeric molecule essential in various biological roles. RNA consists of a single strand of nucleotides (A, C, G, U) that can fold and bond to itself through base-pairings. At first, RNA was regarded as a simple messenger - the conveyor of genetic information from its repository in DNA to the ribosomes. Over the last several decades,

participate in processing of messenger RNAs, to help maintain the telomers of eukaryotic chromosomes, and to influence gene expression in multiple ways (Darnell, 2011; Breaker, 1996; Serganov and Patel, 2007a; Breaker and Joyce, 1994). The specific shape into which RNAs fold plays a major role in their function, which makes RNA folding of prime interest to scientists. An understanding of RNA's three-dimensional structure will allow a greater understanding of RNA function. However, obtaining these

are contact structures with noncrossing arcs when presented as a diagram, see Fig. 1.

The key feature of RNA secondary structures is that they can be inductively constructed¹ (Stein and Everett, 1978). Waterman *et al.* (Waterman, 1978; Stein and Everett, 1978; Nussinov *et al.*, 1978; Kleitman, 1970) studied the combinatorics and folding of RNA secondary structures. The noncrossing arcs of RNA secondary structures allow for a recursive build: let $S_2(n)$ denotes the number of RNA secondary structures over n nucleotides then we have (Waterman, 1978): $S_2(n) = S_2(n-1) + \sum_{j=0}^{n-3} S_2(n-2-j)S_2(j)$, where $S_2(n) = 1$ for $0 \leq n \leq 2$. The recursion forms the basis for more than three decades of research resulting in what can be called the dynamic programming (DP) paradigm. The DP paradigm allows one to compute minimum free energy (MFE) structure in $O(n^3)$ time and $O(n^2)$ space. Implementations of these DP folding algorithms are *mfold* and *ViennaRNA* (Zucker and Stiegler, 1981; Hofacker *et al.*, 1994), employing the energy values derived in (Mathews *et al.*, 1999; Turner and Mathews, 2010). The so called inverse folding, i.e., identifying sequences that realize a given structure as MFE-structure, has been studied in (Hofacker *et al.*, 1994; Busch and Backofen, 2006).

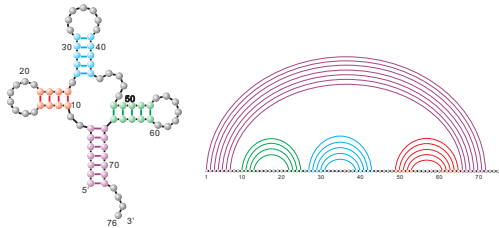


Fig. 1. tRNA: secondary structure and diagram representation.

MFE folding naturally induces a genotype-phenotype (sequence to structure) map, in which the preimage of a structure is called the *neutral network*. Neutral networks are closely related to the *neutral theory* of Motoo Kimura (Kimura, 1968), which stipulates that evolution is driven by mutations that do not change the phenotype. The properties of neutral networks as subsets of sequences in sequence space allow one to study how genotypes evolve. Neutral networks have been studied theoretically via random graph theory (Reidys, 1997), in the context of the molecular quasispecies (Reidys *et al.*, 1997) and by exhaustive enumeration (Grüner *et al.*, 1996; Göbel, 2000). A neutral network represents the set of all inverse folding solutions of a fixed structure. Graph properties, like for instance, size, density and connectivity are of crucial functionality in molecular evolution. Clearly, a vast, extended neutral network is more accessible than small, localized one and on a connected and dense neutral network, neutral evolution can easily be facilitated via point- and pair-mutations. On such a network, a population of RNA sequences can explore sequence space via gradual genotypic changes while maintaining its phenotype.

However, there is more to sequences and structures than MFE-folding: certain RNA sequences exhibit multiple, distinctively different, stable configurations (Baumstark *et al.*, 1997; Schultes and Bartel, 2000), as for example, riboswitches (Serganov and Patel, 2007b; Mandal and Breaker, 2004). Recently (Rezazadegan *et al.*, 2017) evolutionary trajectories, so called *drift walks* have been considered that are obtained by either neutral evolution or switching between a multiplicity of MFE-structures present at a fixed sequence. Such sequences indicate that it may not suffice to

entire RNA energy landscape. Energy landscapes of sequences, i.e., the spectrum of free energies of the associated secondary structures of a fixed sequence have been studied in physics, chemistry, and biochemistry, and play a key role in understanding the dynamics of both RNA and protein folding (Dill *et al.*, 1997; Onuchic *et al.*, 1997; Martinez, 1984; Wolfinger *et al.*, 2004).

In (McCaskill, 1990), McCaskill observed that the tropicalization of the DP routine that computes the MFE-structure produced the partition function of structures for a given sequence. This allows one to study statistical features, as, for instance, base-pairing probabilities of RNA energy landscapes by means of Boltzmann sampling (Tacker *et al.*, 1996; Ding and Lawrence, 2003), enhancing structure prediction (Ding and Lawrence, 2003; Bernhart *et al.*, 2006; Rogers and Heitsch, 2014). Aside from global features, local features are being studied: for instance, local minima of the energy landscape, i.e., ‘energy traps’ are crucial to the understanding of folding dynamics since they represent the metastable configurations (Chen and Dill, 2000; Tinoco and Bustamante, 1999). Statistical features of constrained energy landscapes, corresponding to conditional distributions can also be Boltzmann sampled (Hofacker *et al.*, 1994; Freyhult *et al.*, 2007; Lorenz *et al.*, 2009).

Accordingly, the partition function is tantamount to computing the probability space of structures that a fixed sequence is compatible with. This gives rise to consider the pairing (Barrett *et al.*, 2017):

$$\eta: \mathcal{N}^n \times \mathcal{S}_n \longrightarrow \mathbb{R}, \quad (1)$$

which maps a fixed sequence-structure pair into its free energy. Here \mathcal{N}^n and \mathcal{S}_n denote the space of sequences, σ , and the space of secondary structures, S , respectively. The pairing illuminates the symmetry between sequences and structures, suggesting to consider the ‘dual’ of RNA energy landscape, i.e., the spectrum of free energies of sequences with respect to a fixed structure. This dual has been employed for designing more efficient inverse folding algorithms: (Busch and Backofen, 2006) discovers that using the MFE sequence of a fixed structure as starting point for the inverse folding, significantly accelerates the algorithm. In other words, the global minimum of the RNA dual energy landscape is typically very close in sequence space to the corresponding neutral network. This line of work motivated the use of the dual RNA energy landscape² in inverse folding algorithms (Levin *et al.*, 2012; Garcia-Martin *et al.*, 2016). Recently, (Barrett *et al.*, 2017) proposed a framework considering RNA sequences and their RNA secondary structures simultaneously, as pairs. The RNA dual energy landscape in this context gives rise to an information theoretic framework for RNA sequences.

In practice, the exhaustive exploration of the dual RNA energy landscape is not feasible, whence specific localizations, for instance studying the point-mutant neighborhood of a natural RNA sequence (Borenstein and Ruppin, 2006; Rodrigo and Fares, 2012) have been studied.

To conduct a systematic and biologically meaningful study of the dual RNA energy landscape, we present in this paper an efficient Boltzmann sampling algorithm with a Hamming distance filtration. This filtration facilitates the analysis of Hamming classes of sequences in the dual RNA energy landscape, that would otherwise be impossible to access, see Fig. 3. Instead of being restricted to neighborhoods of point-mutants (Borenstein and Ruppin, 2006; Rodrigo and Fares, 2012), we have now access to arbitrary Hamming classes. Such a dual sampler has to our knowledge first been derived in (Levin *et al.*, 2012). In fact, the sampler arises as the restriction of (Waldispihl *et al.*, 2008), where the structure partition

backbone, lead to a time complexity of $O(h^2 n^3)$, where h and n denote Hamming distance and sequence length, respectively. In contrast, the Boltzmann sampler presented here is based on the loop-decomposition of the fixed structure and has a time complexity of $O(h^2 n)$.

The paper is organized as follows: in Section 2, we discuss our sampling algorithms. In Section 3, we study two application contexts of the dual Boltzmann sampler with the Hamming distance filtration. First we study the inverse fold rate as a function of Hamming distance and then we employ our dual sampler in order to explicitly construct neutral paths in neutral networks.

2 Methods

In (Busch and Backofen, 2006) a minimum free energy (MFE) sequence for a given structure is derived by means of dynamic programming (DP). The algorithm facilitates the arc decomposition of a secondary structure (Waterman, 1978) computing a MFE sequence recursively. In analogy to the partition function of structures, the dual partition function has been computed in (Garcia-Martin *et al.*, 2016; Barrett *et al.*, 2017), where in addition Boltzmann samplers were derived (Garcia-Martin *et al.*, 2016; Barrett *et al.*, 2017).

In this section we introduce an algorithm refining the Boltzmann sampler in (Barrett *et al.*, 2017) that constructs RNA sequences from the Boltzmann ensemble of a structure S , subject to a Hamming distance constraint³. The straightforward approach would be to run a rejection sampler based on the sampler introduced in (Garcia-Martin *et al.*, 2016; Barrett *et al.*, 2017). However, as we shall prove in Section 3, this would result in a rather inefficient algorithm. Instead, we follow a different approach, introducing a new parameter h associated to a subsequence, representing the Hamming distance.

Let us first recall the graph presentation of RNA secondary structures: RNA secondary structures can be represented as diagrams, where vertices are drawn in a horizontal line and arcs in the upper half-plane. In a diagram, vertices are presenting nucleotides and arcs are presenting base-pairs, see Fig. 1. Vertices are labeled by $[n] = \{1, 2, \dots, n\}$ from left to right, indicating the orientation of the backbone from the 5'-end to 3'-end. A base-pair, denoted by (i, j) is an arc connecting vertices labeled by i and j . Two arcs (i, j) and (r, s) are called *crossing* if $i < r, i < r < j < s$, holds. An RNA secondary structure contains exclusively noncrossing arcs and thus induces the partial order: $(r, s) \prec (i, j)$ if and only if $i < r < s < j$.

The energy of a sequence-structure pair $\eta(\sigma, S)$ can be computed as the sum of the energy contributions of individual base-pairs (Nussinov *et al.*, 1978). A more elaborate model (Mathews *et al.*, 1999; Turner and Mathews, 2010) evaluates the total free energy to be the sum of from the energies of loops involving multiple base-pairs. A loop L in a secondary structure is a sequence of intervals $([a_i, b_i])_i, 1 \leq i \leq k$, where $(a_1, b_k), (b_i, a_{i+1}), \forall 1 \leq i \leq k-1$, are base-pairs. Since no crossing arcs are allowed, nucleotides in the interval $([a_i + 1, b_i - 1])_i$ are unpaired. In particular, for $k = 1$, L is called a hairpin loop for $k = 2$ either an interior loop, bulge loop or helix, depending on how many unpaired vertices are contained in the respective intervals, and for $k \geq 3$, a multiloop. Note that the arc (a_1, b_k) is the maximal arc of the loop, i.e., $(b_i, a_{i+1}) \prec (a_1, b_k)$ for all $1 \leq i \leq k-1$, whence L can be represented by (a_1, b_k) . The intersection of two distinct loops is either empty or consists of exactly one base-pair. Each base-pair is contained in exactly two loops and is maximal in exactly one of these two. There is a particular loop, the *exterior*

$(0, n+1)$, referred to as its rainbow and by convention, there are the two "formal" nucleotides N_0, N_{n+1} associated with positions 0 and $n+1$, respectively.

In Turner's energy model, the energy of a loop, $\eta(\sigma, L)$, is determined by its loop type (hairpin, interior loop, exterior loop or multiloop), the specific nucleotide composition of its base-pairs as well as a certain number of unpaired bases contained in it. Those unpaired bases are typically adjacent to a base-pair. Accordingly, the energy of a sequence-structure pair equals the sum of the energies of all the associated loops, i.e.,

$$\eta(\sigma, S) = \sum_{L \in S} \eta(\sigma, L). \quad (2)$$

A secondary structure can be decomposed by successively removing arcs from the outside to the insider (top to bottom), see Fig. 2. Since any base-pair is maximal in exactly one loop, removing a base-pair is tantamount to removing its associated loop.

Viewing a secondary structure, S , as a diagram we observe that any interval $[i, j]$ induces a substructure containing all arcs that have both endpoints contained in $[i, j]$ and denote such substructures by $X_{i,j}^S$. In case the interval $[i, j]$ contains no arcs, we simply refer to the substructure $X_{i,j}^S$ again as an interval. Given S , the concatenation of the two substructures $X_{i,j}^S \cup X_{j+1,k}^S$ is the substructure $X_{i,k}^S$. In the following we shall simply write $X_{i,j}$ instead of $X_{i,j}^S$.

In particular, let (i, j) be a base-pair, L be the loop that is represented by (i, j) and let $S_{i,j}$ be the substructure for which (i, j) is the maximal arc. Suppose $(p_r, q_r), 1 \leq r \leq k$ are base-pairs in L , different from (i, j) , removing the arc (i, j) produces a sequence of substructures $S_{p_1, q_1}, \dots, S_{p_k, q_k}$ as well as a sequence of intervals $[i+1, p_1-1], [q_1+1, p_2-1], \dots, [q_k+1, j-1]$.

Let $q_0 = i$, concatenating the interval $[q_{r-1}+1, p_r-1]$ with S_{p_r, q_r} produces a substructure, which we denote by $M_{q_{r-1}+1, q_r}^r, 1 \leq r \leq k$. Let R_{q_0+1, q_k}^1 be the substructure obtained by concatenating all $M_{q_{r-1}+1, q_r}^r$ for $1 \leq r \leq k$, i.e., $\bigcup_r M_{q_{r-1}+1, q_r}^r$. By construction, removing (i, j) from $S_{i,j}$ generates $R_{q_0+1, q_k}^1 \cup [q_k+1, j-1]$.

Note that R_{q_0+1, q_k}^1 can be obtained by concatenation recursively $M_{q_{r-1}+1, q_r}^r, 1 \leq r \leq k$. We use the superscript w to represent the intermediates (recursively concatenating from right to left):

$$R_{q_{w-1}+1, q_k}^w = \bigcup_{w \leq r \leq k} M_{q_{r-1}+1, q_r}^r.$$

Clearly we have the following bipartition:

$$R_{q_{w-1}+1, q_k}^w = M_{q_{w-1}+1, q_w}^w \bigcup R_{q_w+1, q_k}^{w+1}.$$

This decomposition of secondary structures allows us to compute the partition function efficiently.

Definition 1. Given a structure S and a reference sequence $\bar{\sigma}$, the partition function of S with Hamming distance filtration h to $\bar{\sigma}$ is given by

$$Q_h^{S, \bar{\sigma}} = \sum_{\sigma, d(\sigma, \bar{\sigma})=h} e^{-\frac{\eta(\sigma, S)}{RT}},$$

where $\eta(\sigma, S)$ is the energy of S on σ , $d(\sigma, \bar{\sigma})$ denotes the Hamming distance between σ and $\bar{\sigma}$, R is the universal gas constant and T is the temperature.

In the following we omit the explicit reference to $\bar{\sigma}$ and simply

the partition functions of substructures $X_{a,b}$, $Q_h^{X_{a,b}}(N_a, N_b)$, where $X_{a,b} = S_{a,b}$, $R_{a,b}^w$ or $M_{a,b}^w$, whose left and right endpoints $\sigma_a = N_a$ and $\sigma_b = N_b$ are determined and contributes h to Hamming distance. We consider the set of subsequences

$$\{\sigma_{a,b} \in \mathcal{N}^{b-a+1} \mid d(\sigma_{a,b}, \bar{\sigma}_{a,b}) = h, \sigma_a = N_a, \sigma_b = N_b\},$$

to which we refer to as $\mathcal{S}_h^{a,b}(N_a, N_b)$. Summing over all $\sigma_{a,b} \in \mathcal{S}_h^{a,b}(N_a, N_b)$ we derive

$$Q_h^{X_{a,b}}(N_a, N_b) = \sum_{\sigma_{a,b} \in \mathcal{S}_h^{a,b}(N_a, N_b)} e^{-\frac{\eta(\sigma_{a,b}, X_{a,b})}{RT}}, \quad (3)$$

where $N_a, N_b \in \mathcal{N}$, $\mathcal{N} = \{\mathbf{A}, \mathbf{U}, \mathbf{C}, \mathbf{G}\}$.

We next derive the recursion for $Q_h^{S_{i,j}}(N_i, N_j)$, computed from bottom to top.

Case 1: (i, j) is \prec -minimal, i.e., $S_{i,j}$ is a hairpin loop ($k = 0$). By eq. (3), summing over all subsequence $\sigma_{i,j} \in \mathcal{S}_h^{i,j}(N_i, N_j)$ we derive

$$Q_h^{S_{i,j}}(N_i, N_j) = \sum_{\sigma_{i,j} \in \mathcal{S}_h^{i,j}(N_i, N_j)} e^{-\frac{\eta(\sigma_{i,j}, S_{i,j})}{RT}}.$$

Case 2: (i, j) is non-minimal and $k = 1$, i.e., L is an interior loop. Removing (i, j) produces a single $S_{p,q}$ as well as two intervals $[i+1, p-1]$ and $[q+1, j-1]$, either of which being possibly empty. Suppose $d(\sigma_{i,j}, \bar{\sigma}_{i,j}) = h$ and $d(\sigma_{p,q}, \bar{\sigma}_{p,q}) = t$, where $0 \leq t \leq h$. Then the distance contribution from the intervals $[i+1, p-1]$ and $[q+1, j-1]$, t_1 and t_2 , satisfies $t_1 + t_2 = h - t$. Then $Q_h^{S_{i,j}}(N_i, N_j)$ equals

$$\sum_{t, t_1, t_2} \sum_{N_p, N_q} \sum_{\sigma_{i,p}} \sum_{\sigma_{q,j}} e^{-\frac{\eta(\sigma_{i,j}, L)}{RT}} Q_t^{S_{p,q}}(N_p, N_q),$$

where $t + t_1 + t_2 = h$, $N_p, N_q \in \mathcal{N}$, $\sigma_{i,p} \in \mathcal{S}_{t_1+\delta_p}^{i,p}(N_i, N_p)$ and $\sigma_{q,j} \in \mathcal{S}_{t_2+\delta_q}^{q,j}(N_q, N_j)$. Here $\delta_x = 1$ if $N_x = \bar{\sigma}_x$, and $\delta_x = 0$, otherwise, for $x = p, q$.

Case 3: (i, j) is non-minimal and $k \geq 2$, i.e., L is a multiloop. In this case (in difference to the interior loops analyzed above) the Turner energy model allows us to further decompose the energy of $\eta(\sigma, L)$ into independent components, which in turn allows us to compute $Q_h^{S_{i,j}}(N_i, N_j)$ via recursive bipartitioning. Removing (i, j) produces R_{q_0+1, q_k}^1 as well as $[q_k + 1, j - 1]$, see Fig. 2 (A). The energy $\eta(\sigma_{i,j}, S_{i,j})$ is then given by

$$\eta(\sigma, R_{q_0+1, q_k}^1) + \alpha_{\text{mul}} + \eta_{\text{mul}}((i, j)) + \eta_{\text{mul}}([q_k + 1, j - 1]),$$

where α_{mul} is the energy contribution of forming a multiloop, $\eta_{\text{mul}}((i, j))$ is the energy contribution of base-pair (i, j) in a multiloop, and $\eta_{\text{mul}}([q_k + 1, j - 1])$ is the energy contribution from the unpaired base interval in a multiloop. The sum of the latter three component is denoted by η^0 .

Suppose $d(\sigma_{q_0+1, q_k}, \bar{\sigma}_{q_0+1, q_k}) = t$ and $d(\sigma_{i,j}, \bar{\sigma}_{i,j}) = h$. Then the distance contribution from the unpaired interval $[q_k + 1, j - 1]$ is $h - t - \delta_i - \delta_j$. Then $Q_h^{S_{i,j}}(N_i, N_j)$ equals

$$\sum_t \sum_{N_{q_0+1}, N_{q_k}} \sum_{\sigma_{q_k, j}} e^{-\frac{\eta^0}{RT}} Q_t^{R_{q_0+1, q_k}^1}(N_{q_0+1}, N_{q_k}),$$

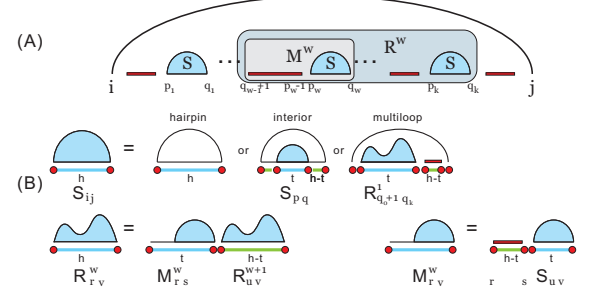


Fig. 2. (A): the substructures $S_{a,b}$, $M_{a,b}^w$ and $R_{a,b}^w$. (B) structural decomposition and Hamming distance distribution.

For notational convenience we set $r = q_{w-1} + 1$, $s = q_w$, $u = q_w + 1$ and $v = q_k$. Suppose $d(\sigma_{r,s}, \bar{\sigma}_{r,s}) = t$ and $d(\sigma_{r,v}, \bar{\sigma}_{r,v}) = h$, then $d(\sigma_{u,v}, \bar{\sigma}_{u,v}) = h - t$. We obtain for $Q_h^{R_{r,v}^w}(N_r, N_v)$ the expression

$$\sum_t \sum_{N_s, N_u} Q_t^{M_{r,s}^w}(N_r, N_s) Q_{h-t}^{R_{u,v}^w}(N_u, N_v),$$

where $0 \leq t \leq h$ and $N_s, N_u \in \mathcal{N}$.

The substructures $M_{q_{w-1}+1, q_w}^w$ are concatenations of $[q_{w-1} + 1, p_w - 1]$ and S_{p_w, q_w} , for $1 \leq w \leq k$. For notational convenience we set $r = q_{w-1} + 1$, $s = p_w - 1$, $u = p_w$ and $v = q_w$.

Suppose $d(\sigma_{u,v}, \bar{\sigma}_{u,v}) = t$ and $d(\sigma_{r,v}, \bar{\sigma}_{r,v}) = h$, then the Hamming distance of $[r, s]$ to the corresponding $\bar{\sigma}$ -interval is $h - t$.

Summing over $0 \leq t \leq h$, all $N_{p_w-1}, N_{p_w} \in \mathcal{N}$, all $\sigma_{q_{w-1}+1, p_w-1} \in \mathcal{S}_{h-t}^{q_{w-1}+1, p_w-1}(N_{q_{w-1}+1}, N_{p_w-1})$, we derive for $Q_h^{M_{r,v}^w}(N_r, N_v)$

$$\sum_t \sum_{N_s, N_u} \sum_{\sigma_{r,s}} Q_{h-t}^{S_{u,v}}(N_u, N_v) e^{-\frac{\eta^w}{RT}},$$

where $0 \leq t \leq h$, $N_s, N_u \in \mathcal{N}$, $\sigma_{r,s} \in \mathcal{S}_{h-t}^{r,s}(N_r, N_s)$ and $\eta^w = \eta_{\text{mul}}((u, v)) + \eta_{\text{mul}}([r, s])$. Here $\eta_{\text{mul}}((u, v))$ is the energy contribution of base-pair (u, v) in a multiloop and $\eta_{\text{mul}}([r, s])$ is the contribution of segment of unpaired bases in a multiloop. We present the recursions in Fig. 2 (B).

The introduction of the intermediate substructures $M_{q_{w-1}+1, q_w}^w$ and $R_{q_{w-1}+1, q_k}^w$ avoids processing concatenation of substructures simultaneously, which would result in a $O(h^{k-1})$ time complexity. The family of intermediate substructures $M_{q_{w-1}+1, q_w}^w$ and $R_{q_{w-1}+1, q_k}^w$ remedies this problem by executing one concatenation at each step, effectively bipartitioning and requiring a time complexity of $O(h)$. In total we encounter $k - 1$ such bipartition, resulting in a $(k - 1)O(h)$ time complexity. Since there are $O(n)$ base-pairs in a structure and each entails to compute $O(h)$ partition functions, we have to consider $O(hn)$ partition functions. As a result the time complexity of the algorithms is $O(h^2n)$.

Following this recursion, $Q_h^{S_{i,j}}(N_i, N_j)$ can be computed from bottom to top as claimed. The recursion terminates, when reaching the rainbow, $(0, n + 1)$. The partition function of S with Hamming distance filtration h to $\bar{\sigma}$ is given by $Q_h^S = Q_h^{S_0, n+1}(N_0, N_{n+1})$, where N_0 and N_{n+1} are ‘‘formal’’ nucleotides, discussed above.

Having computed the partition function $Q_h^{S, \bar{\sigma}}$, we implement the

following the partial order \prec from top to bottom until reaching the hairpin loops.

Since the time complexity of computing a loop energy in Turner’s model is constant, the worst case time complexity of the sampling process is $O(n^2)$ (Ding and Lawrence, 2003), and applying the Boustrophedon technique for Boltzmann sampling, introduced in (Ponty, 2008; Nebel *et al.*, 2011), reduces the time complexity to $O(n \log n)$ on average.

3 Results

In this section, we first study the Hamming distance distribution of sequences generated via the unrestricted dual sampler Barrett *et al.* (2017). We perform this analysis for natural sequences as well as random sequences. The resulting distribution shows that a simple rejection sampler is rather inefficient and motivates the algorithm derived in Section 2.

Here we apply the refined Boltzmann sampler in order to gain deeper insight into IFR and neutral paths. First, given a sequence-structure pair, $(\bar{\sigma}, S)$ we study the rate at which sampled sequences, filtered by Hamming distance, fold into S . Secondly, we apply the sampler in order to develop an efficient heuristic that constructs paths within neutral networks, i.e., given two sequences, both of which folding into a fixed structure S , we identify a path consisting of sequences all of which folding into S , such that two consecutive sequences on the path differ only by a point- or pair-mutations.

Hamming distance distribution: we consider 12 sequence-structure pairs from the human microRNA let-7 family in miRBase (Kozomara and Griffiths-Jones, 2013). For each pair we sample 5×10^4 sequences using the unrestricted sequences sampler in (Barrett *et al.*, 2017). Then we compute the Hamming distance distribution to the natural sequence of the sampled sequences. The distances are normalized by sequence length. We display in Fig. 3 the distance distribution of three distinguished sequence-structure pairs, whose mean distance is in some sense minimal, typical, and maximal, respectively. The full spectrum of these distributions is presented in the SM, Fig. 1.

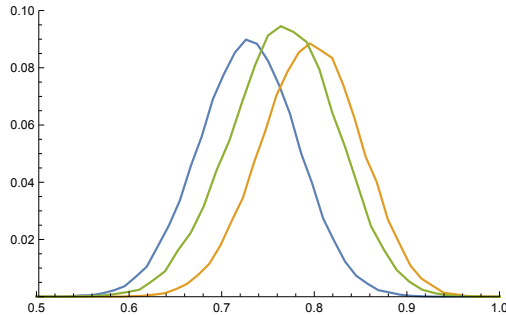


Fig. 3. Hamming distance distribution of sampled sequences for three sequence-structure pair of the human microRNA let-7 family (hum01, hum09, and hum10). For each pair we sample 5×10^4 sequences, using the unrestricted sampler in (Barrett *et al.*, 2017). We display the Hamming distance distribution of the sampled sequences to the natural sequence. The x -axis is the Hamming distance normalized by the sequence length, and the y -axis is frequency sampled sequences.

The data show that the sampled sequences have distances between 60% and 90% of the sequence length to the reference sequence. The mean distance is 70% to 80% of the sequence length, indicating that the unrestricted sampler in (Barrett *et al.*, 2017) does not produce the full

spectrum of sequences. The sampled sequences still have a Hamming distance of 60% to 90% of the sequence length. However, we observe some variations of the distribution, whence we have not only a dependence on structure, but also on the reference sequence. This implies the sampled sequences are not uniformly distributed. More interestingly, we observe that the Hamming distance distribution corresponds to the natural sequence is the least concentrated around the mean.

Inverse fold rate: we study now the inverse fold rate (IFR) of the sampled sequences with respect to different sequence-structure pairs, for different Hamming distances. We associate an indicator variable to each sampled sequence: taking the state 1 if the sequence actually folds into the reference structure and 0, otherwise. By construction the IFR is the mean of this random variable and we consider the IFR of a sequence-structure pair as a function of the Hamming distance, h , to the reference sequence, $\text{IFR}(h)$.

Given a sequence-structure pair $(\bar{\sigma}, S)$, we sample 5×10^4 sequences from S having a fixed Hamming distance, h , where h is ranging from 1 to 20. Then $\text{IFR}(h) = U/M$ where U is the number of sampled sequences folding back to S and M is the sample size.

We consider the microRNA let-7 family of three species: human (hum01-12), lizard (liz01-11) and drosophila (dro01-08), computing their IFRs respectively. We display the mean⁴ IFR of the three species in Fig. 4 and the IFR distributions of individual pairs within the three species in the SM, Fig. 4, Fig. 5 and Fig. 6, respectively.

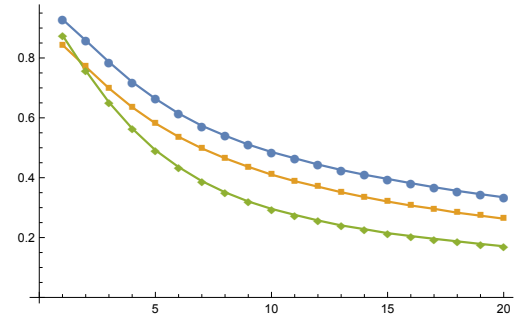


Fig. 4. Mean IFR of sequence-structure pairs of microRNA let-7 family of human (blue), lizard (yellow) and drosophila (green). The x -axis represents Hamming distance and the y -axis represents the IFR.

The Fig. 4 shows that human has the highest, mean IFR while drosophila has the lowest. In addition, the mean IFR decreases for human significantly slower than for drosophila. To analyze robustness and dependencies of these findings, we compute the IFR of random sequence-structure pairs and to those of natural pairs. In the following we restrict ourselves to the hum04 sequence-structure pair. We first consider random sequences compatible with the hum04-structure and thereby create new sequence-structure pairs. Then we compute $\text{IFR}(5)$ of these pairs by sampling 5×10^4 sequences of Hamming distance 5. The $\text{IFR}(5)$ is almost zero for these random sequences indicating that random compatible sequences have little or no connection with the hum04-structure. To identify sequences that are closer related to the hum04-structure, we use our sampler, creating 100 sequence-structure pairs by sampling sequences from the natural pairs of distance 5, 7, 10 and 20, respectively. Then we combine the newly sampled sequences with the hum04-structure, creating

by their IFR(5) in increasing order, see Fig. 5. For reference purposes we display IFR(5) of the natural sequence-structure pair as a dashed line.

Fig. 5 shows that IFR(5) of the natural sequence-structure pair is above the 95 percentile, i.e., better than almost all of the newly created pairs. Furthermore, there exists very few pairs such that $\text{IFR}(5) \in [0.1, 0.3]$ holds. The proportion of sequence having high IFR(5), i.e., $\text{IFR}(5) > 0.3$ drops when the sampled sequence have higher Hamming distance. This finding suggests that the natural pair is locally optimal.

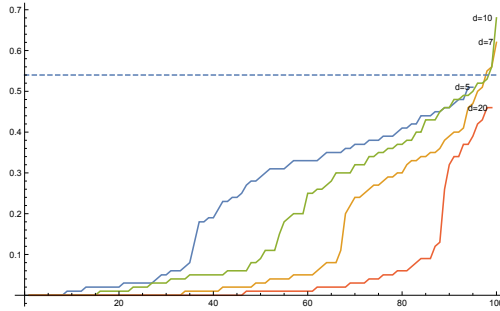


Fig. 5. IFR(5) of the natural sequence-structure pair versus adjacent sampled sequences. We compare the natural sequence-structure pair of hum04 and sample 100 sequences of distance 5, 7, 10 and 20, respectively. We display IFR(5) of the induced sequence-structure pairs sorted by their IFR(5) in increasing order for distance 5 (blue), 7 (yellow), 10 (green) and 20 (red). IFR(5) of the natural sequence-structure pair is displayed as the dashed line. Here the x -axis is labeled by the sorted sequence-structure pairs and the y -axis represents the IFR.

Neutral paths: as discussed in Section 1, connectivity is of central importance in neutral networks. Combined with some form of density, it allows genotypes to explore, by means of point- or pair-mutations, extended portions of sequence space. An exhaustive analysis of connectivity is not feasible even for relatively short sequence length, whence the explicit construction of specific paths within the neutral network is the best possible outcome. To be clear, let us first specify the neutral path problem:

Given two sequences σ_1 and σ_2 , both folding into the structure S , identify a path $\sigma_1 = \tau_0, \tau_1, \dots, \tau_k = \sigma_2$, such that

(*) for all τ_i , $0 \leq i \leq k$, folds to S ,

(**) τ_{i+1} is obtained from τ_i by either a compatible point- or a base-pair mutation.

The construction of such “neutral paths” has been studied in (Göbel and Forst, 2002) using a proof idea that facilitates the construction of neutral paths, for fixed, finite distance d , in random induced subgraphs. However (Göbel and Forst, 2002) exhaustively checks whether such paths are neutral or not, irrespective of d , a task that becomes impracticable for large d . At present, there is no efficient way of finding neutral paths in a neutral networks induced by folding algorithms, in particular in case of the distance between the two sequences being large. In the following we shall employ our sampling algorithm in order to derive an efficient heuristic to solve the neutral path problem.

Certainly, given σ_1 and σ_2 , both folding into S , one can always construct a path between them using the two above moves. By construction this is a S -compatible path. Furthermore, there exists a minimum number

shortest neutral path. In the context of the neutral path problem, we do not require the paths to be minimal in length.

Case 1: $d(\sigma_1, \sigma_2) \leq 5$. Here we exhaustively search all shortest S -compatible paths between σ_1 and σ_2 and check for neutrality. Note that we always have $d_S \leq d$, thus in the worst case, we need to check $5! = 120$ different paths and fold $2^5 = 32$ different sequences. This is feasible for sequence lengths shorter than 10^3 nucleotides, using standard secondary structure folding algorithms (Zuker and Stiegler, 1981; Hofacker *et al.*, 1994).

Case 2: $d(\sigma_1, \sigma_2) > 5$. Suppose σ_1 and σ_2 have Hamming distance h . We sample m sequences from σ_1 with respect to S with distance filtration $h/2$. $m = 1000$ typically suffices but higher sampling size can easily be realized if the IFR is too low. We then select such a sequence with minimum Hamming distance to σ_2 , denoted by τ_s . We have $d(\sigma_1, \tau_s) = h/2 = h_1$ and $d(\tau_s, \sigma_2) = h_2$, where $h_1 + h_2 \geq h$. If $h_2 > h$ we claim the process fails and we conclude we can not find a neutral path between σ_1 and σ_2 . Otherwise, we repeat the process between σ_1 and τ_s , and between τ_s and σ_2 , differentiating Case 1 and Case 2. We show the flow of the algorithm in Fig. 6.

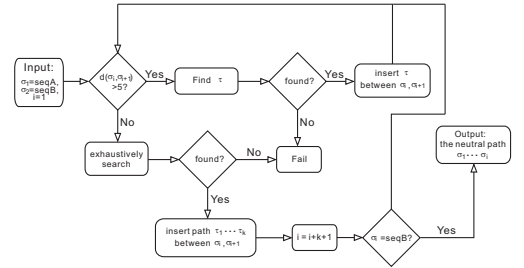


Fig. 6. The algorithm.

The process either fails at some point of the iteration or produces recursively a neutral path. We illustrate a particular neutral path, connecting the natural sequence of hum08 to a Hamming distance 20 sequence in Fig. 7.

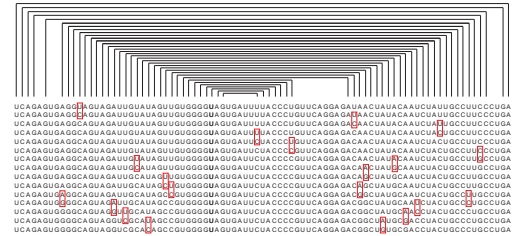


Fig. 7. A neutral path connecting the natural sequence of hum08 to a sequence having Hamming distance 20. All sequences along the path fold into the natural structure of hum08. This particular path has length 14 and consists of 8 point- and 6 base-pair mutants.

As for algorithmic performance: for hum04 we consider the natural sequence and structure pair and sample 100 sequences of Hamming distance 20, 19 of which being neutral. We pair each of these with the natural sequence and compute a neutral path. The algorithm succeeded 18

53 neutral sequences: the algorithm succeeds 49 times and fails in four instances.

For a low level organism microRNA, bra01, which is a Branchiostoma micro RNA, at distance 20, we find 22 neutral sequences: 16 successes and 6 fails.

4 Discussion

The problem of finding a sequence that folds into a given structure, S , has first been studied in (Hofacker *et al.*, 1994). The algorithm consists of two parts: first it constructs a random S -compatible sequence and secondly it performs an adaptive walks of point mutant in the sequence such that facilitates identifying a sequence that folds into S . In this process, neither an inverse fold solution is guaranteed nor the number of adaptive walks required is understood. (Busch and Backofen, 2006) shows that such adaptive walks can be constructed much more easily, when proper care is taken where the process actually initiates. Namely, choosing the S -compatible sequence such that it minimizes the free energy with respect to S . (Levin *et al.*, 2012; Garcia-Martin *et al.*, 2016) observe that Boltzmann sampled sequences exhibit a distinctively higher rate of folding again into S .

The high IFR of sampled sequences from a structural ensemble is not only useful in finding candidate sequences for inverse folding problems reflects in some sense the robustness of the structure. High IFR in structural ensembles indicate that the structure is likely preserved within limited energy change and mutations on a sequence. This is quite subtle as competing structural configurations may offer a fixed sequence an even lower and thus more preferable free energy. The problem can therefore not be reduced to minimizing free energy of sequences with respect to a fixed structure, it is context dependent.

However, sampled sequences from the structural ensemble are not conserved and differ vastly from each other. It is natural to bring evolutionary trajectories into the picture, necessitating the ability to study Boltzmann sampled sequences having fixed Hamming distance to some reference sequence. This allows us to investigate local features and brings sequence information into the picture. By introducing the Hamming distance filtration, we can zoom into a specific sequence as well as its neighborhood in the structural ensemble. These sequences are not only sorted by the given structure but also evolutionary close to the reference sequence. This approach shifts focus to considering sequences and structures as pairs, as discussed in (Barrett *et al.*, 2017)

(Levin *et al.*, 2012) presents a Boltzmann sampler of sequences from a structural ensemble with Hamming distance restriction. The algorithm described in (Levin *et al.*, 2012) constitutes a constrained version of the algorithm described in (Waldspühl *et al.*, 2008), having a time complexity of $O(h^2n^3)$ where h is the Hamming distance. The partition function of sequences with distance filtration on all secondary structures is computed, requiring to consider all subintervals of $[1, n]$ as well as an additional for-loop index, induced by the concatenation of two substructures.

Our algorithm has a time complexity of $O(h^2n)$, a result of different recursions. We utilize the hierarchical organization, or equivalently the induced partial order of the arcs of a secondary structure structure, together with the fact that free energy is computed based on loops. This allows us to compute the partition function from the inside to the outside (bottom to top from the tree prospective). The routine is purely driven by the fixed structure, whence no redundant information is computed.

The dual sampler, i.e. the Boltzmann sampler of sequences with

structural diversity of the derived sequences can be analyzed effectively with the enhanced sampler. These studies follow the generalized scheme of inferring information on any random variable over sequences partitioned into Hamming classes. Hamming classes in this sense can be viewed as blocks of a partition to which a random variable can be restricted to. Our analysis of IFR gives first indications that microRNAs of highly evolved organisms exhibit higher robustness than those of organisms of lower level: in the context of evolutionary optimization achieving robustness of evolved phenotypes is an advancement.

The enhanced sampler is furthermore useful for construction neutral paths. The naive approach to identifying neutral paths between two given sequences σ_1 and σ_2 (Göbel and Forst, 2002) is to exhaustively check all shortest compatible paths between them for neutrality. While this is feasible for small d_S is small, as d_S increases, the number of these shortest paths grows hyper-exponential. In addition a neutral path might still exist even when all shortest compatible paths are not neutral. The enhanced sampler shows that even at large Hamming distance, sampled sequence have a high inverse fold rate, provided reference sequence and structure are natural. This motivated the “divide and conquer” strategy employed to construct the neutral paths. We use the enhanced sampler to construct recursively “intermediate” sequences, that are traversed by the neutral path. Iterating this process, we can reduce the Hamming distances to the point where exhaustive search becomes feasible, see Fig. 6 in Section 3.

It is possible that the shortest possible neutral path has length strictly greater than the S -compatible distance, however, Case 1 does not consider any such paths. In order to validate the approach of Case 1, we consider sequence-structure pairs of the microRNA let-7 family across various species (human, cattle lizard and other low level organism, 12 pairs for each class) as the origin. Then for each sequence-structure pair, we identify inverse fold solutions by dual sampling 1×10^4 sequences of Hamming distance 5 and consider all neutral solutions⁵ as the terminus. By exhaustive search, we observe that for all of these sequence pairs, there exists a neutral path, whose length is equal to the S -compatible distance.

5 Acknowledgments

We want to thank Stanley Hefta and Peter Stadler for their input on this manuscript. We gratefully acknowledge the help of Kevin Shinpaugh and the computational support team at BI, Mia Shu, Thomas Li, Henning Mortveit, Madhav Marathe and Reza Rezazadegan for discussions. The fourth author is a Thermo Fisher Scientific Fellow in Advanced Systems for Information Biology and acknowledges their support of this work.

References

- Barrett, C., Huang, F., and Reidys, C. M. (2017). Sequence-structure relations of biopolymers. *Bioinformatics*, **33**(3), 382–389.
- Baumstark, T., Schröder, A. R., and Riesner, D. (1997). Viroid processing: switch from cleavage to ligation is driven by a change from a tetraloop to a loop e conformation. *The EMBO journal*, **16**(3), 599–610.
- Bernhart, S., Tafer, H., Mückstein, U., Flamm, C., Stadler, P., and Hofacker, I. (2006). Partition function and base pairing probabilities of RNA heterodimers. *Algorithms Mol. Biol.*, **1**, 3.
- Borenstein, E. and Ruppin, E. (2006). Direct evolution of genetic robustness in microRNA. *Proceedings of the National Academy of Sciences*, **103**(17), 6593–6598.
- Breaker, R. R. (1996). Are engineered proteins getting competition from rna? *Current Opinion in Biotechnology*, **7**(4), 442–448.
- Breaker, R. R. and Joyce, G. F. (1994). Inventing and improving ribozyme function:

- Busch, A. and Backofen, R. (2006). INFO-RNA—a fast approach to inverse rna folding. *Bioinformatics*, **22**(15), 1823–31.
- Chen, S.-J. and Dill, K. A. (2000). Rna folding energy landscapes. *Proceedings of the National Academy of Sciences*, **97**(2), 646–651.
- Darnell, J. E. (2011). *RNA: life's indispensable molecule*. Cold Spring Harbor Laboratory Press.
- Dill, K. A., Chan, H. S., et al. (1997). From Levinthal to pathways to funnels. *Nature structural biology*, **4**(1), 10–19.
- Ding, Y. and Lawrence, C. E. (2003). A statistical sampling algorithm for RNA secondary structure prediction. *Nucleic Acids Res.*, **31**, 7280–7301.
- Freyhult, E., Moulton, V., and Clote, P. (2007). Boltzmann probability of rna structural neighbors and riboswitch detection. *Bioinformatics*.
- García-Martín, J. A., Bayegan, A. H., Dotu, I., and Clote, P. (2016). RNADualPF: software to compute the dual partition function with sample applications in molecular evolution theory. *BMC Bioinformatics*, **17**(1), 424.
- Göbel, U. (2000). Networks of minimum free energy RNA secondary structures. PhD Theise, University of Vienna.
- Göbel, U. and Forst, C. V. (2002). RNA pathfinder—global properties of neutral networks. *Zeitschrift fuer physikalische Chemie*, **216**(2/2002), 175.
- Grüner, R., Giegerich, R., Strothmann, D., Reidys, C. M., Weber, J., Hofacker, I. L., Stadler, P. F., and Schuster, P. (1996). Analysis of RNA sequence structure maps by exhaustive enumeration I. structures of neutral networks and shape space covering. *Chem. Mon.*, **127**, 355–374.
- Hofacker, I. L., Fontana, W., Stadler, P. F., Bonhoeffer, L. S., Tacker, M., and Schuster, P. (1994). Fast folding and comparison of RNA secondary structures. *Monatsh. Chem.*, **125**, 167–188.
- Kimura, M. (1968). Evolutionary rate at the molecular level. *Nature*, **217**, 624–626.
- Kleitman, D. (1970). Proportions of irreducible diagrams. *Studies in Appl. Math.*, **49**, 297–299.
- Kozomara, A. and Griffiths-Jones, S. (2013). mirbase: annotating high confidence micromRNAs using deep sequencing data. *Nucleic acids research*, **42**(D1), D68–D73.
- Levin, A., Lis, M., Ponty, Y., O'Donnell, C. W., Devadas, S., Berger, B., and Waldspühl, J. (2012). A global sampling approach to designing and reengineering rna secondary structures. *Nucleic acids research*, **40**(20), 10041–10052.
- Lorenz, R., Flamm, C., and Hofacker, I. L. (2009). 2d projections of rna folding landscapes. *GCB*, **157**(11–20), 21.
- Mandal, M. and Breaker, R. R. (2004). Adenine riboswitches and gene activation by disruption of a transcription terminator. *Nature Structural and Molecular Biology*, **11**(1), 29–36.
- Martinez, H. M. (1984). An rna folding rule.
- Mathews, D., Sabina, J., Zuker, M., and Turner, D. (1999). Expanded sequence dependence of thermodynamic parameters improves prediction of RNA secondary structure. *J. Mol. Biol.*, **288**, 911–940.
- McCaskill, J. S. (1990). The equilibrium partition function and base pair binding probabilities for RNA secondary structure. *Biopolymers*, **29**, 1105–1119.
- Nebel, M. E., Scheid, A., and Weinberg, F. (2011). Random generation of RNA secondary structures according to native distributions. *Algorithms Mol. Biol.*, **6**(24), doi:10.1186/1748–7188–6–24.
- Nussinov, R., Piecznik, G., Griggs, J. R., and Kleitman, D. J. (1978). Algorithms for loop matching. *SIAM J. Appl. Math.*, **35**(1), 68–82.
- Onuchic, J. N., Luthey-Schulten, Z., and Wolynes, P. G. (1997). Theory of protein folding: the energy landscape perspective. *Annual review of physical chemistry*, **48**(1), 545–600.
- Ponty, Y. (2008). Efficient sampling of RNA secondary structures from the Boltzmann ensemble of low-energy: the boustrophedon method. *J. Math. Biol.*, **56**(1–2), 107–27.
- Reidys, C. M. (1997). Random induced subgraphs of general n -cubes. *Adv. Appl. Math.*, **19**, 360–377.
- Reidys, C. M., Stadler, P. F., and Schuster, P. (1997). Generic properties of combinatory maps and neutral networks of RNA secondary structures. *Bull. Math. Biol.*, **59**(2), 339–397.
- Rezazadegan, R., Barrett, C., and Reidys, C. (2017). Neutrality and continuity in rna evolution. *to appear in Bioinformatics*.
- Rodrigo, G. and Fares, M. A. (2012). Describing the structural robustness landscape of bacterial small rnas. *BMC evolutionary biology*, **12**(1), 52.
- Rogers, E. and Heitsch, C. E. (2014). Profiling small RNA reveals multimodal substructural signals in a boltzmann ensemble. *Nucl. Acids Res.*, **42**(22), e171.
- Schultes, E. A. and Bartel, D. P. (2000). One sequence, two ribozymes: implications for the emergence of new ribozyme folds. *Science*, **289**(5478), 448–452.
- Serganov, A. and Patel, D. J. (2007a). Ribozymes, riboswitches and beyond: regulation of gene expression without proteins. *Nature reviews. Genetics*, **8**(10), 776.
- Serganov, A. and Patel, D. J. (2007b). Ribozymes, riboswitches and beyond: regulation of gene expression without proteins. *Nat. Rev. Genet.*, **10**, 776–790.
- Stein, P. and Everett, C. (1978). On a class of linked diagrams ii. asymptotics. *Discrete Mathematics*, **21**(3), 309–318.
- Tacker, M., Stadler, P. F., Bornberg-Bauer, E. G., Hofacker, I. L., and Schuster, P. (1996). Algorithm independent properties of RNA structure prediction. *Eur. Biophys. J.*, **25**, 115–130.
- Tinoco, I. and Bustamante, C. (1999). How rna folds. *Journal of molecular biology*, **293**(2), 271–281.
- Turner, D. and Mathews, D. H. (2010). NNDB: the nearest neighbor parameter database for predicting stability of nucleic acid secondary structure. *Nucl. Acids Res.*, **38**(Database), 280–282.
- Waldspühl, J., Devadas, S., Berger, B., and Clote, P. (2008). Efficient algorithms for probing the rna mutation landscape. *PLoS computational biology*, **4**(8), e1000124.
- Waterman, M. S. (1978). Secondary structure of single-stranded nucleic acids. *Adv. Math. (Suppl. Studies)*, **1**, 167–212.
- Wolfinger, M. T., Svrcek-Seiler, W. A., Flamm, C., Hofacker, I. L., and Stadler, P. F. (2004). Efficient computation of rna folding dynamics. *Journal of Physics A: Mathematical and General*, **37**(17), 4731.
- Zuker, M. and Stiegler, P. (1981). Optimal computer folding of larger RNA sequences using thermodynamics and auxiliary information. *Nucleic Acids Res.*, **9**, 133–148.